2011-10-05

Supported Monoethanolamine for CO2 Separation

Morris D. Argyle
mdargyle@byu.edu

Zhuoyan Sun

See next page for additional authors

Original Publication Citation
Z. Sun, M. Fan, M.D. Argyle, "Supported Monoethanolamine for CO2 Separation." Industrial & Engineering Chemistry Research, 5, 11343-11349, 211.

Supported Monoethenalamine for CO_2 Separation

Zhuoyan Sun[§], Maohong Fan[§] and Morris Argyle[§, ζ]

[§] *Department of Chemical & Petroleum Engineering, University of Wyoming, Laramie, WY 82071*

[ζ] *Department of Chemical Engineering, Brigham Young University, Provo, UT 84602*

ABSTRACT

An alternative method for using monoethenalamine (MEA) in CO_2 separation is developed from the viewpoints of the MEA-CO_2 reaction environment and the process of spent sorbent regeneration. The method could be used to considerably reduce energy consumption compared to conventional aqueous MEA processes. MEA-TiO_2 (MT) CO_2 sorbent is synthesized using pure MEA and a support material, TiO_2. The performance of the MT sorbent on CO_2 separation was investigated in tubular reactors under various experimental conditions. The effects of several major factors on CO_2 sorption by the MT sorbent were investigated. The sorption capacity of the MT sorbent increased with MEA loading, reaching 48.1 mg-CO_2/g-MT at 45 wt% MEA. However, an optimum of 40 wt% MEA loading was chosen for most of the sorption tests conducted in this research. Temperature affected the CO_2 sorption capacity considerably, with optimum values of 45°C for adsorption and 90°C for regeneration, while humidity had a small positive effect under initial test conditions. In addition to TiO_2, $TiO(OH)_2$ and FeOOH were also tested as potential supports for MEA. $TiO(OH)_2$ appears to be the best support material for

MEA, but more evaluation is needed. The MT sorbent is regenerable, with a multi-cycle sorption capacity of ~ 40 mg-CO_2/g-MT under the given experimental conditions.

INTRODUCTION

The atmospheric CO_2 concentration has increased by almost 38% since the beginning of the industrial revolution to a current level of about 386.8 ppm.[1] More than 30% of all anthropogenic CO_2 emissions are estimated to have resulted from fossil fuel based electricity generation.[2] These fossil fuels, including coal, oil and natural gas, will be used as major energy sources for the foreseeable future due to their low prices and abundance. However, people are concerned about the increase of CO_2 concentration in the atmosphere since CO_2 has been implicated as one of the main greenhouse gases leading to global climate changes. Accordingly, capture of CO_2 from flue gas streams in fossil-fuel based power plants has been considered as one of the major strategies for reduction of anthropogenic CO_2 emissions and thus the potential risks resulting from climate changes.

To date, all commercial CO_2 capture processes have been based on liquid amine compounds. Amine solutions are basic and can chemically remove many acid gases, including CO_2, from flue gas[3]. Among those frequently used amine compounds is monoethanolamine (MEA). Aqueous amines along with membranes have been successfully used for separation CO_2 from natural gas; however, they have not been used in fossil fuels based power plants since the overall costs associated with the current technologies are too high to be acceptable. The high costs are mainly due to use of large concentrations of water in the aqueous amine solutions made for carbon dioxide separation. Typical amine solutions used by the natural gas industry for gas cleaning can contain as much as 70 wt% water.[4,5]

In recent years, people are increasingly interested in using solid sorbents synthesized with amines and solid supports or grafting materials for CO_2 capture in power plants. Different support materials[6-8] have been used for immobilization of amines. Compared to aqueous amines, solid sorbents have several advantages when used for separation of CO_2 from flue gases in power plants.[9-11] Firstly, solid amine sorbents require less energy than aqueous amines for separation of the same amount of CO_2 since they avoid energy needed to heat and evaporate H_2O, with its high specific-heat-capacity and latentheat of vaporization, in aqueous amine solutions during sorbent regeneration or CO_2 stripping processes. Secondly, they are easy to handle and transport. In addition, they are less problematic than aqueous amine solutions from an operational viewpoint because they are less corrosive.

Unlike traditionally immobilized amine based CO_2 sorbents, the pure MEA in the sorbent developed in this research is immobilized during the CO_2 sorption phase, but is mobilized during CO_2 desorption phase. More specifically, immobilized MEA reacts with CO_2 in a sorption rector, but is transported to another reactor during the CO_2 desorption process due to the difference in sorption and desorption temperatures. The MEA utilization approach studied in this research is expected to reduce CO_2 separation energy consumption. Several major factors potentially affecting the CO_2 sorption capacities of the MEA utilization method were investigated. The results obtained in the research could be used for further development or optimization of the MEA based CO_2 separation technology.

EXPERIMENTAL SECTION

TiO_2 preparation and characterization

The support material (TiO_2) used in this research was prepared with $Ti(OC_2H_5)_4$ (99 wt%, Acros) containing 33-35 wt-% TiO_2. The first preparation step was to add a predetermined amount of $Ti(OC_2H_5)_4$ to water with a H_2O:$Ti(OC_2H_5)_4$ molar ratio of 26.3, followed by stirring for 1 hour. The resulting precipitate was filtered, washed with deionized water, and then dried at 393 K for 1.5 h. TiO_2 was obtained by calcining the resultant $TiO(OH)_2$ in air at 1,023 K for 3 hours.

The prepared TiO_2 powder was characterized with a Micromeritics TriStar 3000 V6.04 A nitrogen physisorption analyzer to determine surface areas by the BET (Brunauer, Emmett, and Teller) method. Powder X-ray diffraction (XRD) of TiO_2 was performed on a Philips X'Pert diffractometer using Cu-Kα radiation under the following operating conditions: voltage, 40 kV; current, 40 mA; start angle, 10°; end angle, 90°; step size, 0.01°; time per step, 0.05 s; and scan speed, 0.02. The experimental data were digitally collected and recorded.

Each MEA-TiO_2 (MT) sorbent was prepared by loading a certain amount of as-purchased MEA (99 wt%, Acros) onto the prepared TiO_2. Five MEA:TiO_2 mass ratios or MEA loadings were used for preparing the MT sorbents tested for this research. The best loading was determined and used for all subsequent tests.

Apparatus

The experimental set-up used for the CO_2 separation tests is shown in Figure 1. It has three parts: a gas preparation unit, a CO_2 sorption/desorption system, and gas-phase CO_2 concentration analysis equipment. Dilute CO_2 from cylinder 1 (1 mol% CO_2 in 99 mol% N_2) was used for the sorption tests. N_2 from cylinder 2 (100 mol%) was used for CO_2 desorption tests and cleaning the apparatus. The flow rates of the inlet gases were controlled by two flow meters (Matheson Tri-gas FM-1050, labeled 3' and 3''). An additional flow meter (3''') was used to measure the flow rate of the whole system.

Sorption tests were performed in the bottom reactor (11'), which has an inner diameter and length of 9 mm and 610 mm, respectively. The sorbent bed (9) was prepared by loading MT sorbent between two bed holders (8) made from quartz wool. The bottom reactor (11') was held in a tube furnace (10, Thermo Corporation, TF55030A-1), where its temperature was controlled (7, Yokogawa M&C Corporation, UT150). A syringe pump (4) was used to generate the water vapor used in moisture-containing gas streams. Temperature controlled (6, MiniTrol, Glas-Col Inc.) thermo-tapes (5) heated the inlet gas tubes to prevent condensation of water vapor prior to entering the bottom reactor. The effluent gas stream from the bottom reactor passed through a sorbent bed (12, consisting of the support material for MT sorbent, which was generally TiO_2) in the top reactor (11'') to condense the MEA vaporized from the bottom reactor using cooling water circulating through a spiral copper pipe (13, inner diameter: 1.5 mm) and held at 12°C by a small refrigeration unit (14, MGW Lauda, RC-20 controller). The effluent gas from the top reactor (11'') entered a water removal unit (15) and then an infrared gas analyzer (16, ZRE, Fuji Electric System Co. Ltd.). The sorption profiles were collected by a data collection computer (17).

CO_2 sorption/desorption

Each CO_2 desorption test was started immediately after the bed was saturated with CO_2, as determined when the outlet CO_2 concentration during a sorption step became equal to the inlet CO_2 concentration. During a desorption step, pure N_2 from cylinder (1) was used as the carrier gas to bring the desorbed CO_2 from the bottom reactor (11') through top reactor (11'') and finally to the gas analyzer (16). MEA vapor resulting from the CO_2 desorption in the bottom reactor (11') also flowed into the top reactor (11'') and condensed there. Desorption temperatures were controlled by the bottom temperature controller (7). When CO_2 desorption was completed, the material in the bottom rector (11') was pure TiO_2 because all MEA was transported to the top reactor (11'') and formed MT sorbent with the TiO_2 there due to the condensation of the MEA vapor from the bottom reactor (11') on the surface of pure TiO_2 originally in the top reactor (11''). Then the positions of the top and bottom reactors were switched to start the next sorption-desorption cycle.

3. Results and Discussion

3.1 Characterization of TiO_2

The BET surface area, pore average size and volume of the sorbent support material, TiO_2, are 5.68 m^2/g, 66.4 nm and 0.11 cm^3/g, respectively. The obtained TiO_2 X-ray diffraction pattern is shown in Figure 2. Three major diffraction peaks appear at 2θ

values of 27.5°, 36.2°, and 54.4°, corresponding to diffraction from the (110), (101), and (211) crystal planes, respectively, which are consistent with TiO_2 in the rutile phase.[12,13]

3.2 Factors affecting CO_2 sorption

3.2.1 MEA loading and distribution on TiO_2

The relationship between MEA loading on the surface of TiO_2 and CO_2 sorption capacity of synthesized MT sorbent is shown in Figure 3. The CO_2 sorption capacity of the MT sorbent increases with the MEA loading and reaches 48.1 mg-CO_2/g-MT when the MEA loading percentage is 45 wt% under the given experimental conditions.

The increasing trend in Figure 3 resulting from the reaction between CO_2 and pure MEA (instead of aqueous amine solution) can be understood through the following equations[14]

$$\begin{aligned} & Q_g \frac{dC_{CO_2}}{d(W_{MEA,0} - w_{MEA})} - kC_{CO_2}^{n_{CO_2}} \beta_{MEA}^{m_{MEA}} \\ & = -Q_g \frac{dC_{CO_2}}{dw_{MEA}} - kC_{CO_2}^{n_{CO_2}} \beta_{MEA}^{m_{MEA}} \\ & = 0 \end{aligned} \tag{E1}$$

$$-\frac{d\alpha_{MEA}}{dt} = k_d C_{CO_2}^{n_{CO_2}} \beta_{MEA}^{m_{MEA}} \tag{E2}$$

where Q_g is the volumetric flow rate of the inlet gas mixture, $W_{MEA,0}$ is initial loading of MEA on TiO_2, C_{CO_2} is the concentration of CO_2 in outlet gas stream at any sorption time (t), k is the initial CO_2 sorption rate constant, k_d is the deactivation rate constant of pure MEA on the surface of TiO_2, n_{CO_2} is the reaction order with respect to CO_2, and m_{MEA} is the exponent value of β_{MEA}. In E1 and E2, β_{MEA} is the activity of MEA, which ranges from 0 to 1, and can be defined as

$$\beta_{MEA} = \frac{W_{MEA,0} - w_{MEA,\mathrm{t}}}{W_{MEA,0}} \qquad \text{(E3)}$$

where $w_{MEA,t}$ is the quantity of MEA consumed at reaction time t.

According to the zwitterion mechanism for the reaction between MEA and CO_2, both n_{CO_2} and m_{MEA} in E1 and E2 should be 1.[15] Then, combining the integrated forms of E1 and E2 leads to[14]

$$C_{CO_2} = C_{CO_2,0} \exp\{[1 - \exp(kW_{MEA,0}(1 - \exp(-k_d t))/Q_g)]\exp(-k_d t)\}/[1 - \exp(-k_d t)]. \quad \text{(E4)}$$

E4 clearly shows that higher initial loading of MEA on TiO_2 results in lower outlet CO_2 concentration (C_{CO_2}) and thus higher CO_2 sorption capacity of MT. However, C_{CO_2} is also affected by other parameters, such as k and k_d in E1, E2 and E4. The values of k and k_d are determined by various factors including the surface area, particle size, and pore structure of TiO_2, and the distribution of MEA on the TiO_2. Therefore, the characteristics of TiO_2 affect its CO_2 sorption profiles considerably, although the relationship was not investigated as part of this research.

MEA is well-known for its reactivity with CO_2, which was also observed in this study. Typically, the MT sorbent could achieve one half of its total capacity within 10 minutes under any test conditions used in this research. However, much longer periods of time were needed to attain the full capacity of an MT sample. The average CO_2 adsorption rate of the supported sorbent in the first 5 minutes is ~ 8 mg-CO_2/g-MT/min, indicating that CO_2 is readily able to react with MEA on the surface of the sorbent. However, MEA molecules far away from the surface of MT sorbent (close to the surface of the support TiO_2 particles) or condensed in the TiO_2 pores are not easily accessible to CO_2 due to diffusion limitations. This explains why the CO_2 sorption capacity did not improve much when MEA loading on the MT sorbent increases from 40 to 45 wt%, as observed in Figure 3. Therefore, 40 wt% MEA loading was chosen to evaluate the effect of all the other factors on CO_2 sorption.

3.2.2 Moisture

The MT sorbent was developed to overcome the shortcoming of conventional aqueous MEA-based CO_2 separation technologies by eliminating the use of water while maintaining its advantage of strong CO_2 absorption. However, the effect of water on the CO_2 sorption of MT has to be considered since flue gas from all combustion processes, including coal-fired power plants, contain water despite the MT sorbent being made without water. Therefore, a gas containing 0 vol% H_2O, 1.0 vol% CO_2 and 99 vol% N_2 and another gas with 1.0 vol% CO_2 and 99.0 vol% N_2 were compared for their CO_2 sorption profiles. The results are shown in Figure 4, which shows the CO_2 break through curves for these two gases. Generally speaking, moisture shows a positive effect on CO_2 sorption, especially in the initial CO_2 sorption period in which CO_2 outlet concentration is lower than 0.1 vol% (curve B). The performance of MT in this time period is important since it determines the breakthrough capacity of the sorbent.

The CO_2 sorption mechanisms with and without the presence of water are expected to be different. Within a humid environment, the associated MEA-CO_2 reaction mechanism based on the zwitterions theory proposed by Danckwerts[3] and developed by others[11, 15, 16] can be written as

$$2H_2O \xleftrightarrow{k_{R1}} OH^- + H_3O^+ \tag{R1}$$

$$CO_2 + 2H_2O \xleftrightarrow{k_{R2}, k_{-R2}, K_{R2}} HCO_3^- + H_3O^+ \tag{R2}$$

$$HCO_3^- + H_2O \xleftrightarrow{K_{R3}} CO_3^{2-} + H_3O^+ \tag{R3}$$

$$CO_2 + RNH_2 \xleftrightarrow{k_{R2}, k_{-R4}, K_{R4}} RNH_2^+COO^- \tag{R4}$$

$$RNH_2^+COO^- + RNH_2 \xleftrightarrow{k_{R5}, k_{-R5}, K_{R5}} RNH_3^+ + RNHCOO^- \tag{R5}$$

$$RNH_2^+COO^- + H_2O \xleftrightarrow{k_{R6}, k_{-R6}, K_{R6}} H_3O^+ + RNHCOO^- \tag{R6}$$

$$RNH_2^+COO^- + OH^- \xleftrightarrow{k_{R7}, k_{-R7}, K_{R7}} H_2O + RNHCOO^- \tag{R7}$$

$$RNHCOO^- + H_2O \xleftrightarrow{k_{R8}, k_{-R8}, K_{R8}} RNH_2 + HCO_3^- \tag{R8}$$

$$RNH_3^+ + H_2O \xleftrightarrow{k_{R9}, k_{-R9}, K_{R9}} RNH_2 + H_3O^+ \tag{R9}$$

$$CO_2 + OH^- \xleftrightarrow{k_{R10}, k_{-R10}, K_{R10}} HCO_3^- \tag{R10}$$

$$RNH_2^+COO^- + HCO_3^- \xleftrightarrow{k_{R11}, k_{-R11}, K_{R11}} H_2CO_3 + RNHCOO^- \tag{R11}$$

$$RNH_2^+COO^- + CO_3^{2-} \xleftrightarrow{k_{R12}, k_{-R12}., K_{R12}} HCO_3^- + RNHCOO^- \tag{R12}$$

$$2RNH_2 + CO_2 \xleftrightarrow{k_{R13}, k_{-R13}} [(RNH_3)^+(R\ NHCOO)^-] \tag{R13}$$

$$RNH_2 + CO_2 + H_2O \xleftrightarrow{k_{R14}, k_{-R14}} [(RNH_3)^+(HCO_3)^-] \tag{R14}$$

where k_i , k_{-i}, and K_i are the forward reaction rate constant, the reverse reaction rate constant, and the equilibrium constant of the reversible reactions, *i*, respectively. The reaction rate of CO_2 can be expressed as[11, 15, 17]

$$r_{CO_2-MEA} = \frac{[CO_2][RNH_2] - \frac{k_{-4}}{k_4}[RNHCOO^-]\frac{\sum k_{-b}[BH^+]}{\sum k_b[B]}}{\frac{1}{k_4} + \frac{k_{-4}}{k_4\sum k_b[B]}} \tag{E5}$$

where B represents the species which can abstract the proton from the zwitterion, including [H_2O], and k_b and k_{-b} are the forward and reverse reaction rate constants of the reverse reactions involving B. However, according to their experimental data and derivations, many researchers[17, 18] proposed that the zwitterion reaction scheme based CO_2 sorption rate can be written as

$$r_{CO_2-MEA} = k_4[CO_2][RNH_2] \qquad \text{(E6)}$$

where r_{CO_2-MEA} is not a function of water concentration. Ramachandran et al.[15] concluded that E5 is more representative than E6 for the kinetics of MEA based CO_2 sorption within a humid environment, although they demonstrated that E5 needs to be modified. The data in Figure 4 is in accordance with their finding. The results in Figure 4 also agree with the kinetic model of Crooks and Donnellan[17, 19] using a termolecular mechanism

$$\mathrm{r}_{\mathrm{CO_2-MEA}} = -\left\{\mathrm{k}_{\mathrm{RNH_2}}[\mathrm{RNH_2}] + \mathrm{k}_{\mathrm{H_2O}}[\mathrm{H_2O}][\mathrm{RNH_2}][\mathrm{CO_2}]\right\} \qquad \text{(E7)}$$

in which k_{RNH_2} and k_{H_2O} are the corresponding rate constants with respect to RNH_2 and H_2O.

Furthermore, the degree to which water concentration affects r_{CO_2-MEA} may need to be reconsidered. According to E7, the CO_2-MEA reaction is first order with respect to both H_2O and CO_2. However, the data in Figure 4 do not support this conclusion since water did not show such a large positive effect. Actually, the effect decreases, disappears and finally becomes slightly negative as the sorption process proceeds. Therefore, the kinetics associated with the reactions in dry and wet

environments may need further polishing.

3.2.3 Sorption temperature

Effects of sorption temperature on the total CO_2 sorption capacity of MT sorbents were evaluated in the temperature range of 25-65℃. Figure 5 shows the CO_2 break through curves for each of these conditions.. The CO_2 sorption capacity increases with temperature in the range of 25 to 45°C, but decreases with the further increases of temperature from 45 to 65°C.

The relationship between T and CO_2 sorption capacity can be understood from the thermodynamic and kinetic characteristics of R13. R13 is an exothermic reaction[20, 21] or its enthalpy change ($\Delta H_{R13} < 0$) is negative under the experimental conditions. Based on the van't Hoff relationship,[22] temperature increases do not favor R13 since equilibrium CO_2 sorption capacity (determined by K_{R13} and associated with K_{R4} and K_{R5}) decreases due to the negative ΔH_{R13}

$$\frac{d\ln K_{R13}}{dT} = \frac{d\ln K_{R4}K_{R5}}{dT} = \frac{\Delta H_{R13}}{RT^2}. \qquad \text{(E8)}$$

Two methods can be used for calculation of K_{R13} for MT-based CO_2 sorption in a dry environment at a given temperature, T. The first is based on the thermodynamic properties of MEA, CO_2, $[(RNH_3)^+(R\ NHCOO)^-]$ in R13 using

$$\Delta G^o_{R13} = -RT\ln K_{R13} = \Delta H^o_{0,\mathrm{R13}} - \frac{T}{T_0}(\Delta H^o_{0,R13} - \Delta G^o_{0,\mathrm{R13}}) + \Delta C^o_P(T-T_0) - T\Delta C^o_P \ln\frac{T}{T_0} \qquad \text{(E9)}$$

where T_0 is reference temperature, ΔH_0^o and ΔG_0^o are the standard enthalpy and free Gibbs energy changes of R13 at the reference temperature, and

$$\Delta C_P^o = C_{P,\mathrm{[(RNH3)+(R\ NHCOO)-]}}^o - 2\, C_{P,\mathrm{RNH_2}}^o - C_{P,\mathrm{CO_2}}^o \tag{E10}$$

where $C_{P,\mathrm{[(RNH3)+(R\ NHCOO)-]}}^o$, $C_{P,\mathrm{RNH_2}}^o$ and $C_{P,\mathrm{CO_2}}^o$ represent the heat capacities of the three reactants and products at constant pressure. The second method is to combine E8 with the following relationship

$$\begin{aligned} K_{R13} &= K_{R4} K_{R5} \\ &= \frac{k_{R4}}{k_{-R4}} \frac{k_{R5}}{k_{-R5}} \end{aligned} \tag{E11}$$

where k_{R4}, k_{-R4}, k_{R5} and k_{-R5} are the forward and reverse rate constants of reactions R4 and R5.

The forward reaction rate constants, k_{R4} and k_{R5}, increase with T according to the Arrhenius equation[23] while K_{R13} in E8 and E11 decreases with T. Therefore, an optimal CO_2 sorption temperature exists that is a compromise between these kinetic and thermodynamic factors to obtain a reasonably high rate of R13 and yet large CO_2 sorption. In other words, the optimal sorption temperature for the MT based CO_2 sorption technology is defined as that which maximizes the CO_2 sorption capacity within a given reaction time period. The optimal temperature at which the maximum total CO_2 adsorption capacity was achieved under the given experimental conditions is 45°C.

3.2.4 Desorption temperature

CO_2 desorption tests were performed at 80°C, 90°C, 100°C and 110°C to evaluate the effect of temperature on CO_2 sorption capacity of the MT sorbent regenerated for next cycle of sorption and desorption. The results are shown in Figure 6. The intermediate temperatures, 90°C and 100°C, are better based on the sorption capacities obtained in the next sorption-desorption cycle. However, due to the higher energy consumption at 100°C, 90°C was chosen as the CO_2 desorption temperature for all other MT evaluation tests.

3.2.5 Alternative support materials for MEA

An alternative Ti based support material is $TiO(OH)_2$, which can be easily prepared at low temperatures compared to TiO_2. It is stable even at 400°C.[24] Its performance as a support for MEA is better than TiO_2 to some degree during most of the sorption period, as shown in CO_2 break through curves in Figure 7. The fact might be explained with the kinetic model obtained by Ramachandran et al.[15] They found that the OH^- increases the reaction rate between MEA and CO_2. Therefore, $TiO(OH)_2$ can probably accelerate CO_2 sorption to some degree due to the OH^- in its structure.

Among many other possible highly porous and inexpensive MEA support materials is FeOOH. FeOOH starts to dehydrate at 213°C or 490 K.[25] Therefore, it is thermally stable under the operation conditions used in this research. It also has OH^- in its structure and is less expensive than TiO_2 and $TiO(OH)_2$. The sorption results with the pure MEA supported with FeOOH is also shown in Figure 7. FeOOH is better than TiO_2, but not as good as $TiO(OH)_2$. When choosing support materials for MEA, other factors should also be considered. For example, acidic compounds in the flue gas, SO_x and NO_x, may affect the life spans of the support materials due to their potential reactions with the acidic compounds. Ti based compounds are better than FeOOH from the perspective of their corrosion-resistance abilities. Therefore, comprehensive comparisons should be made when a support material is selected for synthesis of future MEA-based CO_2 separation sorbents.

3.3 Sorbent regeneration

Industrial chemisorbents are required not only to be highly active and selective, but also regenerable. Therefore, five-cycle CO_2 sorption-desorption tests with MT sorbents were run under conditions with and without moisture. The results are presented in Figures 8A and 8B. The average adsorption capacities for five-cycle tests at 45°C under dry and humid (1 vol% H_2O) sorption conditions are 45.8 and 48.1 mg-CO_2/g-MT, respectively, indicating MT can be used in both dry and wet environments for effective CO_2 separation.

The capacities of MT under the two different environments are higher than that of aqueous MEA, which can absorb 36 mg-CO_2/g-aqueous-MEA.[26] In addition, they are also higher than the CO_2 sorption capacities of 21 sorbents among 24 evaluated by Sjostrom and Krutka in 2010.[27, 28] Most of those 24 sorbents contain 40-50 wt% amines, which is equal to or higher than the MEA percentage (40 wt%) of the MT sorbent used in this research. The regeneration temperatures of those sorbents varied from 80 to 120°C and increased by 10°C with each subsequent sorption-desorption cycle compared to the constant 90°C used for the spent MT regeneration. The quantities of CO_2 immobilized on MT during the sorption period and CO_2 desorbed from spent MT during the desorption process, determined by integrating CO_2 concentration change profiles in each sorption-desorption cycle, are very close. In other words, the working capacity, as defined by Sjostrom and Krutka,[28] is almost equal to sorption capacity for the MT sorbent. This is the reason that the CO_2 sorption capacities do not fluctuate considerably from one sorption-desorption cycle to another, as shown in Figures 8A and 8B.

The amount of energy needed for regeneration of a spent sorbent is an important consideration in its applicability, and can be evaluated by the following equation[28, 29]

$$\frac{Q}{m_c} = \frac{m_e}{m_c} \cdot C_e \cdot \Delta T + \frac{B}{L} \cdot C_s \cdot \Delta T + C_{p.c} \cdot T_2 - C_s \cdot T_1 + \frac{Q_r}{m_c}$$

where 1 and 2 stand for the CO_2 sorption and regeneration states, respectively, the subscripts, e, s, and c respectively represent the equipment, the sorbent, and the CO_2, m is the mass, C is the specific heat, C_p is the constant pressure heat capacity for CO_2, Q is the heat input, Q_r is the heat of reaction, B is a constant of proportionality with dimensional units, and L is the CO_2 loading capacity, defined as mole-CO_2/kg sorbent. To reduce energy consumption needed for MT sorbent regeneration, more effort needs to made to increase L, which can be realized by exploring better support materials and optimizing CO_2 sorption conditions.

4. Conclusion

The MT sorbent can be prepared using a simple method in an environmentally benign manner since no additional chemicals, such as organic solvents, are needed. The equipment requirements for separation of CO_2 with the MT based technology should not be as demanding as those associated with the majority of other CO_2 separation technologies since spent sorbent regeneration temperature is 90°C, lower or much lower than those needed for other technologies,[28] with no external addition of water to the sorption system. Therefore, the capital equipment investment needed for the MT based CO_2 separation technology should be low.

Operational costs account for the majority of the overall CO_2 separation costs in all CO_2 capture technologies, with CO_2 desorption typically being the most expensive step. Avoidance of use of water and the reduction of CO_2 desorption temperature should contribute significantly to the total cost reduction of CO_2 separation.

However, much more work needs to be done before the MT based CO_2 separation process can be industrialized. For example, the mechanism of the positive effect of OH^- on CO_2 sorption capacity needs to be further understood. In addition, studies on the thermodynamics and kinetics of R13 are still lacking, even though those of R14 are well-researched. R13 and R14 have different reactants and products. Therefore, the thermodynamic and kinetic study results reported in the literature for R14 can not be used for R13. Actually, even for R14, many disagreements exist among the published papers regarding its thermodynamic and kinetic properties under the same CO_2 sorption conditions. For example, the enthalpy change of R14 during CO_2 sorption at 320 K is reported by Palmeri et al.[20] as ~57 kJ/mole-CO_2, while Mathonat et al.[30] report the value as ~80 kJ/mole-CO_2. Finally, the overall costs of using MT for CO_2 separation should be systematically compared to other amine-based CO_2 sorption technologies.

ACKNOWLEDGEMENTS

This research was supported by the School of Energy Resource at the University of Wyoming and the Department of Energy.

REFERENCES

1. http://www.wmo.int/pages/prog/arep/gaw/ghg/GHGbulletin.html World Meteorological Organization (WMO), 2010, WMO greenhouse gas bulletin. No. 6.

2. http://www.ieaghg.org/index.php?/20091218110/what-is-css.html IEA Greenhouse Gas R&D Programme. CO_2 capture and storage.

3. Danckwerts, P. V., Reaction of CO_2 with ethanolamines. *Chemical Engineering Science* **1979,** 34, (4), 443-446.

4. Abu-Zahra, M. R. M.; Schneiders, L. H. J.; Niederer, J. P. M.; Feron, P. H. M.; Versteeg, G. F., CO_2 capture from power plants. Part I. A parametric study of the technical-performance based on monoethanolamine. *International Journal of Greenhouse Gas Control* **2007,** 1, (1), 37-46.

5. Feng, B.; Du, M.; Dennis, T. J.; Anthony, K.; Perumal, M. J., Reduction of Energy Requirement of CO_2 Desorption by Adding Acid into CO_2-Loaded Solvent. *Energy & Fuels* **2010,** 24, 213-219.

6. Tanaka, H., Comparison of thermal-properties and kinetics of decompositions of $NAHCO_3$ and $KHCO_3$. *Journal of Thermal Analysis* **1987,** 32, (2), 521-526.

7. Glasscock, D. A.; Critchfield, J. E.; Rochelle, G. T., CO_2 absorption desorption in mixtures of methyldiethanolamine with monoethanolamine or diethanolamine. *Chemical Engineering Science* **1991,** 46, (11), 2829-2845.

8. Hagewiesche, D. P.; Ashour, S. S.; Alghawas, H. A.; Sandall, O. C., Absorption of carbon-dioxide into aqueous blends of monoethanolamine and n-methyldiethanolamine. *Chemical Engineering Science* **1995,** 50, (7), 1071-1079.

9. Mandal, B. P.; Guha, M.; Biswas, A. K.; Bandyopadhyay, S. S., Removal of carbon dioxide by absorption in mixed amines: modelling of absorption in aqueous MDEA/MEA and AMP/MEA solutions. *Chemical Engineering Science* **2001,** 56, (21-22), 6217-6224.

10. Liao, C. H.; Li, M. H., Kinetics of absorption of carbon dioxide into aqueous solutions of monoethanolamine plus N-methyldiethanolamine. *Chemical Engineering Science* **2002,** 57, (21), 4569-4582.

11. Ramachandran, N.; Aboudheir, A.; Idem, R.; Tontiwachwuthikul, P., Kinetics of the absorption of CO_2 into mixed aqueous loaded solutions of monoethanolamine and methyldiethanolamine. *Industrial & Engineering Chemistry Research* **2006,** 45, (8), 2608-2616.

12. Wilska, S., An X-ray diffraction study to determine the effect of the method of preparation upon the crystal structure of TiO_2. *Acta Chemica Scandinavica* **1954,** 8, (10), 1796-1801.

13. Cheng, T. C.; Yao, K. S.; Hsieh, Y. H.; Hsieh, L. L.; Chang, C. Y., Optimizing preparation of the TiO_2 thin film reactor using the Taguchi method. *Materials & Design* **2010,** 31, (4), 1749-1751.

14. Park, S. W.; Sung, D. H.; Choi, B. S.; Oh, K. J.; Moon, K. H., Sorption of carbon dioxide onto sodium carbonate. *Separation Science and Technology* **2006,** 41, (12), 2665-2684.

15. Aboudheir, A.; Tontiwachwuthikul, P.; Chakma, A.; Idem, R., Kinetics of the reactive absorption of carbon dioxide in high CO_2-loaded, concentrated aqueous

monoethanolamine solutions. *Chemical Engineering Science* **2003,** 58, (23-24), 5195-5210.

16. Han, B.; Zhou, C.; Wu, J.; Tempel, D. J.; Cheng, H., Understanding CO_2 Capture Mechanisms in Aqueous Monoethanolamine via First Principles Simulations. *Phys. Chem. Lett.* **2011,** 2, 522–526.

17. Versteeg, G. F.; Van Dijck, L. A. J.; Van Swaaij, W. P. M., On the kinetics between CO_2 and alkanolamines both in aqueous and non-aqueous solutions. An overview. *Chemical Engineering Communications* **1996,** 144, 113-158.

18. Blauwhoff, P. M. M.; Versteeg, G. F.; Vanswaaij, W. P. M., A study on the reaction between CO_2 and alkanolamines in aqueous-solutions. *Chemical Engineering Science* **1984,** 39, (2), 207-225.

19. Crooks, J. E.; Donnellan, J. P., Kinetics and mechanism of the reaction between carbon-dioxide and amines in aqueous-solution. *Journal of the Chemical Society-Perkin Transactions 2* **1989**, (4), 331-333.

20. Palmeri, N.; Cavallaro, S.; Bart, J. C. J., Carbon dioxide absorption by MEA - A preliminary evaluation of a bubbling column reactor. *Journal of Thermal Analysis and Calorimetry* **2008,** 91, (1), 87-91.

21. Kim, I.; Svendsen, H. F., Heat of absorption of carbon dioxide (CO_2) in monoethanolamine (MEA) and 2-(Aminoethyl)ethanolamine (AEEA) solutions. *Industrial & Engineering Chemistry Research* **2007,** 46, (17), 5803-5809.

22. Smith, J. M.; Van Ness, H. C.; Abbott, M. M., *Introduction to Chemical Engineering Thermodynamics*. 6 ed.; Ma Graw Hill: 2001.

23. Fogler, H. S., *Elements of Chemical Reaction Engineering*. 4 ed.; Prentice Hall PTR: 2006.

24. Lim, J.; Park, S.; Kang, S., Carbothermal Reduction of TiO(OH)(2) in the Synthesis of (Ti,W)C. *Journal of the American Ceramic Society* **2010,** 93, (4), 937-940.

25. Diakonov, II, Thermodynamic properties of iron oxides and hydroxides. III. Surface and bulk thermodynamic properties of lepidocrocite (γ-FeOOH) to 500 K. *European Journal of Mineralogy* **1998,** 10, (1), 31-41.

26. Chakma, A.; Meisen, A., Methyl-diethanolamine degradation - Mechanism and kinetics. *Canadian Journal of Chemical Engineering* **1997,** 75, (5), 861-871.

27. Khatri, R. A.; Chuang, S. S. C.; Soong, Y.; Gray, M., Carbon dioxide capture by diamine-grafted SBA-15: A combined Fourier transform infrared and mass spectrometry study. *Industrial & Engineering Chemistry Research* **2005,** 44, (10), 3702-3708.

28. Sjostrom, S.; Krutka, H., Evaluation of solid sorbents as a retrofit technology for CO2 capture. *Fuel* **2010,** 89, (6), 1298-1306.

29. Hoffman, J. S.; Richards, G. A.; Pennline, H. W.; Fischer, D.; Keller, G., Factors reactor for dioxide with solid, regenerable sorbents. In *Proceedings of the International Technical Conference on Coal Utilization & Fuel Systems*, 2008; Vol. 2, pp 1139-1150.

30. Mathonat, C.; Majer, V.; Mather, A. E.; Grolier, J. P. E., Use of flow calorimetry for determining enthalpies of absorption and the solubility of CO_2 in aqueous monoethanolamine solutions. *Industrial & Engineering Chemistry Research* **1998,** 37, (10), 4136-4141.

List of Figures

Figure 1. Schematic diagram of the carbon dioxide separation setup (1: N_2 cylinder; 2: CO_2 cylinder; 3'/3''/3''': flow meters; 4: syringe pump; 5: heat tape; 6: temperature controller for heat tape; 7: temperature controller for furnace; 8: quartz wool; 9: sorbent bed; 10: furnace; 11'/11'': bottom reactor/top reactor; 12: sorbent support material (TiO_2/$TiO(OH)_2$/FeOOH); 13: cooling water; 14: cooling water temperature controller; 15: water vapor removal unit; 16: multi-gas analyzer; 17: data collection unit).

Figure 2. X-ray diffraction pattern of the prepared TiO_2.

Figure 3. Effect of MEA loadings on sorption capacity of MT sorbent (CO_2: 1.0 vol%; N_2: 99.0 vol%; gas flow rate: 0.3 L/min; sorption temperature: 45°C).

Figure 4. Effect of moisture [A (H_2O: 0 vol%; MT: 40 wt% MEA loading; CO_2: 1.0 vol%; N_2: 99 vol%; gas flow rate: 0.3 L/min; sorption temperature: 45°C), B (H_2O: 1.0 vol%; MT: 40 wt% MEA loading; CO_2: 1.0 vol%; N_2: 98.0 vol%; gas flow rate: 0.3 L/min; sorption temperature: 45°C)].

Figure 5. Effect of temperature on CO_2 sorption profile (A) and capacity (B) (MT: 40 wt-% MEA loading; CO_2: 1.0 vol%; N_2: 99.0 vol%; gas flow rate: 0.3 L/min; sorption temperature: 45°C).

Figure 6. Effect of desorption temperature (MT: 40 wt% MEA loading; CO_2: 1.0 vol%; N_2: 99 vol%; gas flow rate: 0.3 L/min; sorption temperature: 45°C).

Figure 7. Comparison of different support materials (A: TiO_2; B: $TiO(OH)_2$; C: FeOOH) for their effects on CO_2 sorption (MEA loading in each sorbent: 40 wt%; CO_2: 1.0 vol%; N_2: 99.0 vol%; gas flow rate: 0.3 L/min; sorption temperature: 45°C).

Figure 8 CO_2 sorption capacities of MT during five sorption-desorption cycles [A (sorption gas: CO_2: 1.0 vol%; N_2: 99 vol%), B (sorption gas: H_2O: 1.0 vol%; CO_2: 1.0 vol%; N_2: 98 vol%), sorption (MT: 40 wt-% MEA loading; gas flow rate: 0.3 L/min; sorption temperature: 45°C), desorption (N_2: 100 vol-%; gas flow rate: 0.3 L/min; sorption temperature: 90°C)].

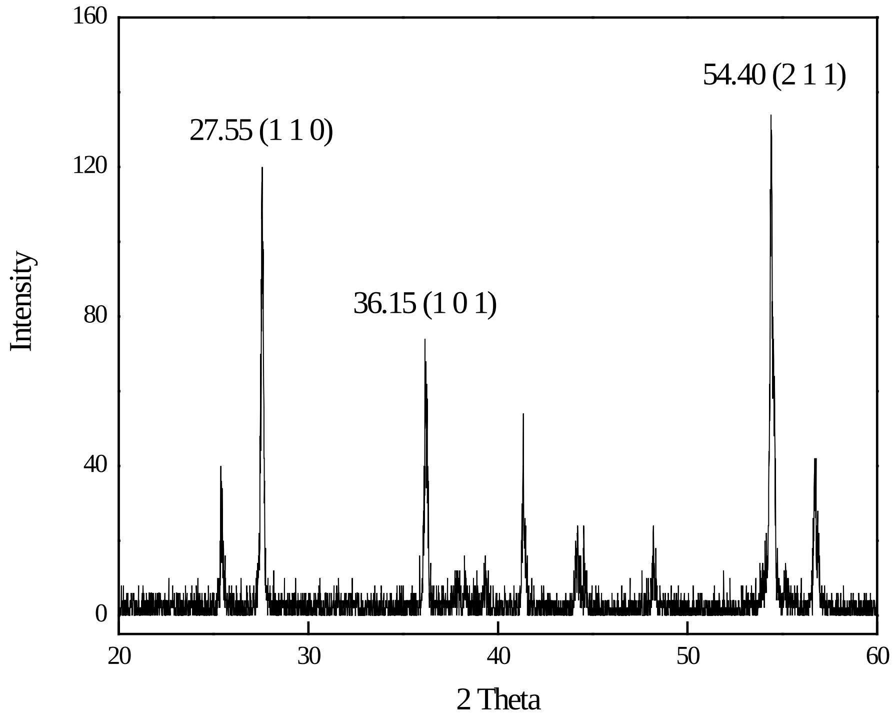

160
120
80
40
0
Intensity
27.55 (1 1 0)
36.15 (1 0 1)
54.40 (2 1 1)
20
30
40
50
60
2 Theta

Figure 2

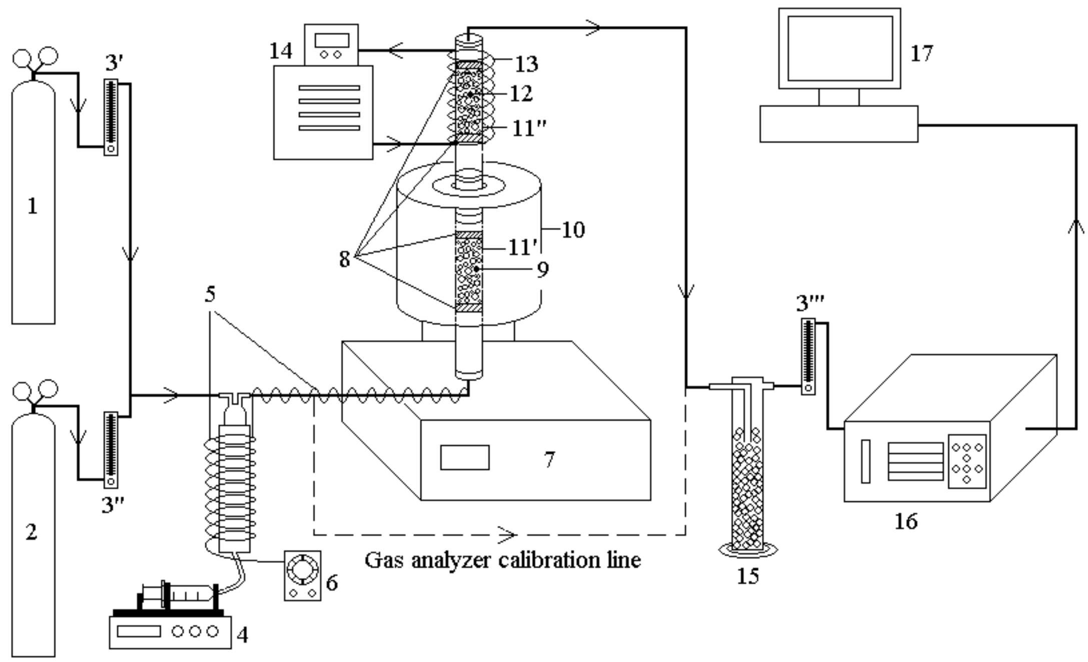
1
2
3′
3″
3‴
4
5
6
7
8
9
10
11′
11″
12
13
14
15
16
17
Gas analyzer calibration line

Figure 1

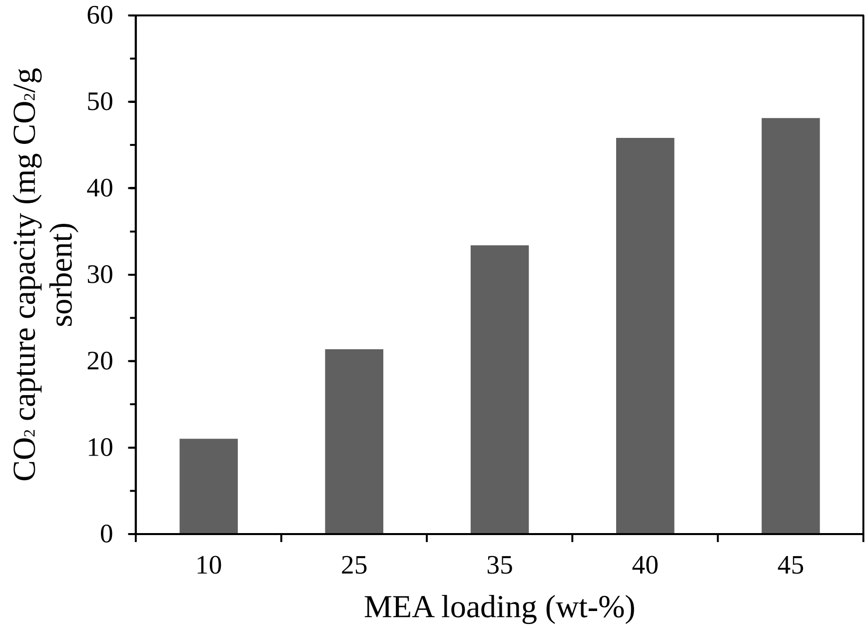
60
50
40
30
20
10
0
CO₂ capture capacity (mg CO₂/g sorbent)
10
25
35
40
45
MEA loading (wt-%)

Figure 3

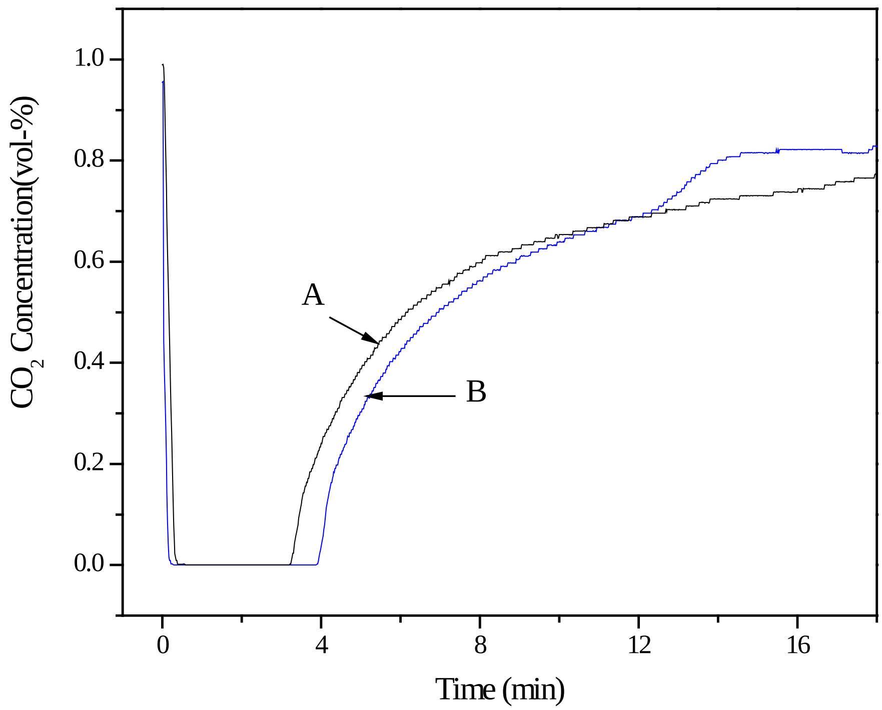

Figure 4

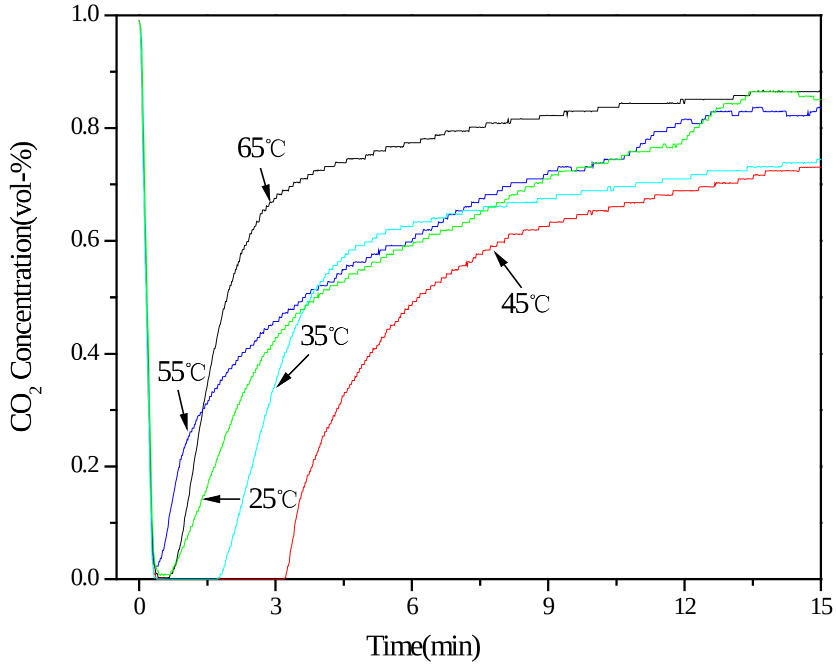

1.0
0.8
0.6
0.4
0.2
0.0
CO2 Concentration(vol-%)
0
3
6
9
12
15
Time(min)
65℃
55℃
35℃
25℃
45℃

(A)

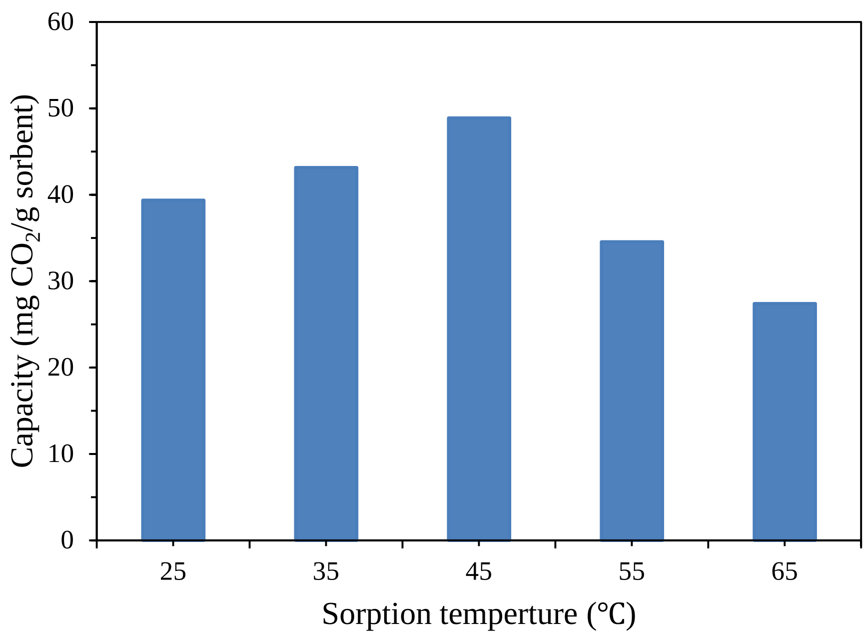

60
50
40
30
20
10
0
Capacity (mg CO2/g sorbent)
25
35
45
55
65
Sorption temperture (°C)

(B)

Figure 5

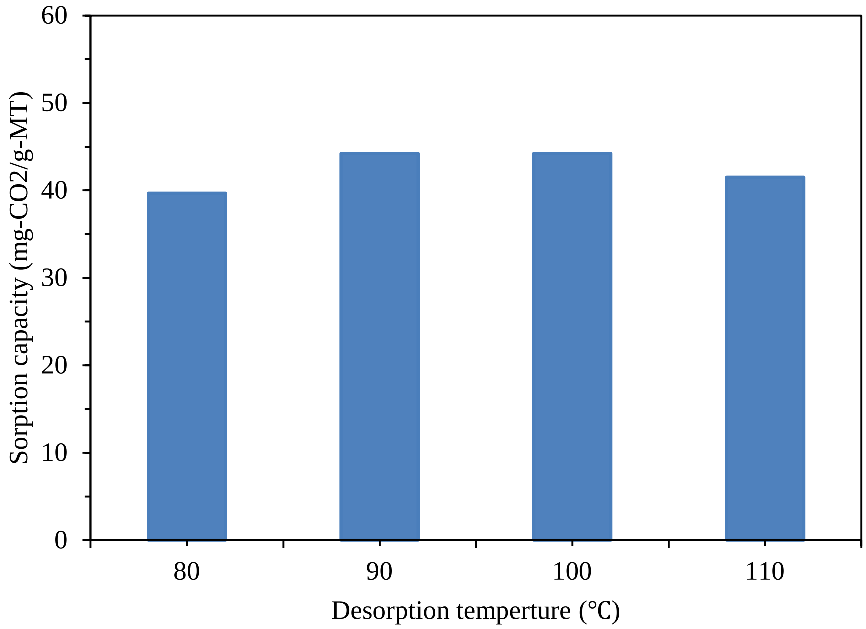
Sorption capacity (mg-CO2/g-MT)
60
50
40
30
20
10
0
80
90
100
110
Desorption temperture (℃)

Figure 6

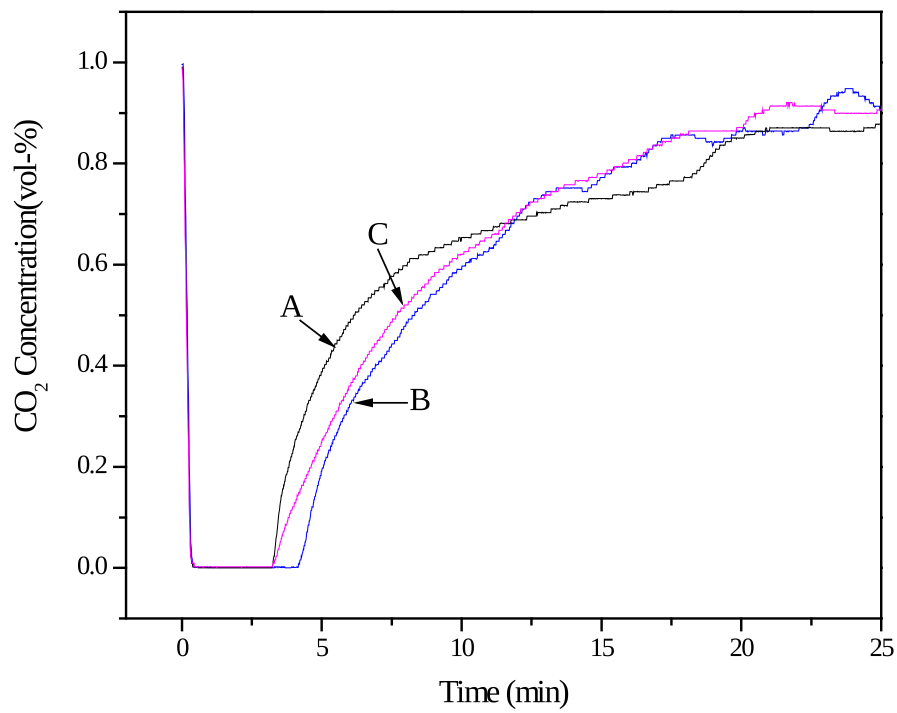

1.0
0.8
0.6
0.4
0.2
0.0
0
5
10
15
20
25
Time (min)
CO_2 Concentration(vol-%)
A
B
C

Figure 7

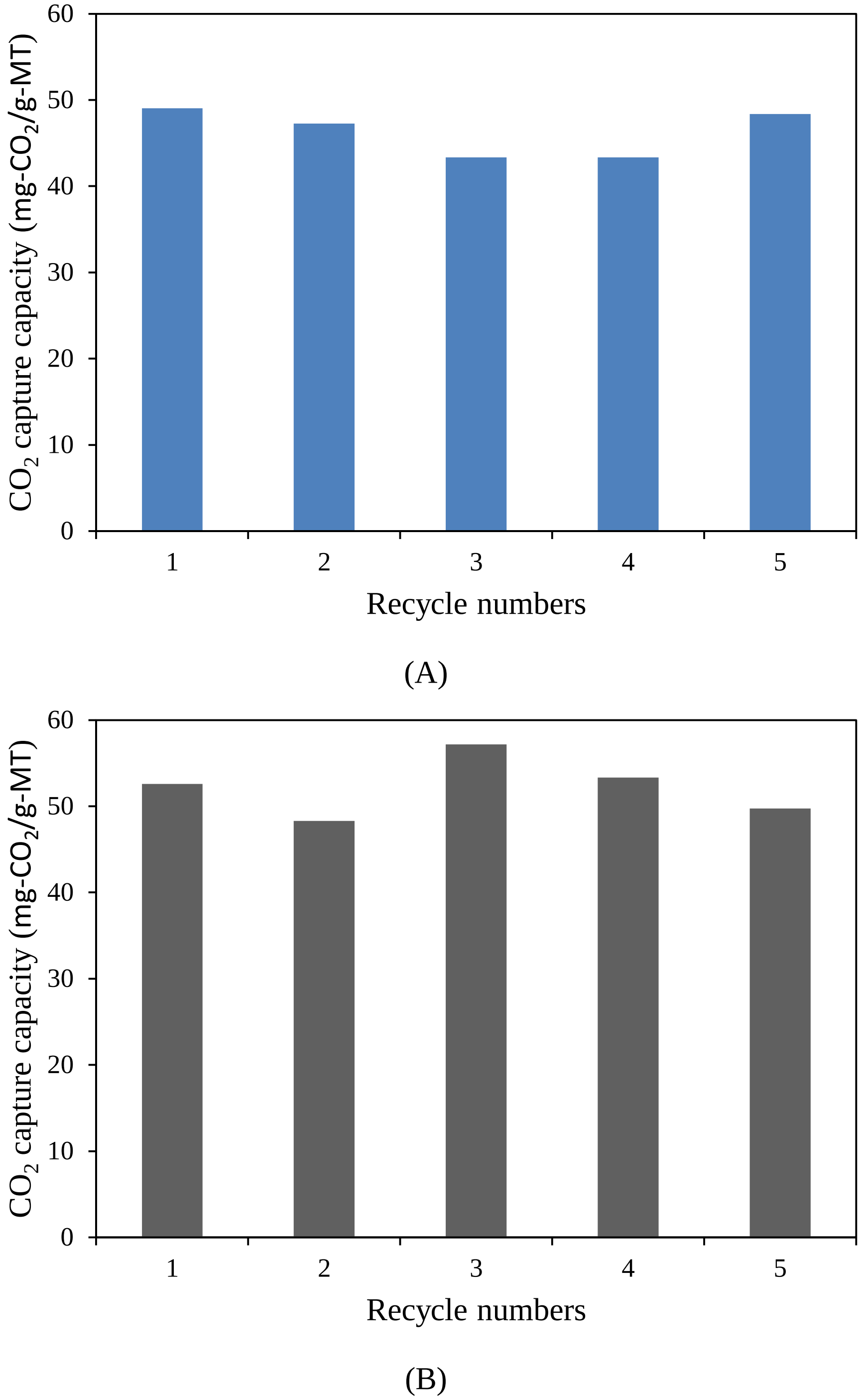
CO2 capture capacity (mg-CO2/g-MT)
60
50
40
30
20
10
0
1
2
3
4
5
Recycle numbers
(A)
CO2 capture capacity (mg-CO2/g-MT)
60
50
40
30
20
10
0
1
2
3
4
5
Recycle numbers
(B)

Figure 8